

# Fabrication and characterization of zinc nitrate doped $\text{TiO}_2$ nanotubes for dye-sensitized solar cells

B. Samran<sup>1</sup> , E.N. Timah<sup>2</sup> , T Phatungthane<sup>1</sup> , P. Thongpanit<sup>1</sup> , B. Kadroon<sup>1</sup> ,

S. Photharin<sup>3</sup> , S. Chaiwichian<sup>4</sup> 

<sup>1</sup> Nakhon Phanom University, Nakhon Phanom, Thailand

<sup>2</sup> Trinity International School, Bangkok, Thailand

<sup>3</sup> Kasetsart University, Sakonnakhon, Thailand

<sup>4</sup> Rajamangala University of Technology Isan, Sakonnakhon, Thailand

saranyou530531117@gmail.com

## ABSTRACT

Zinc-doped titanium dioxide nanotubes were successfully synthesized, characterized, and tested as materials for energy conversion in dye-sensitized solar cells. The  $\text{TiO}_2$  nanotubes were grown through single-face anodization at a constant direct current voltage of 50 V and room temperature on titanium sheets with a thickness of 0.25 mm and purity of 99.7 %. The electrolyte was composed of ethylene glycol, ammonium fluoride (0.3 % wt.  $\text{NH}_4\text{F}$ ), and deionized water (2 % v/v  $\text{H}_2\text{O}$ ). The titania nanotubes were doped with Zn using  $\text{Zn}(\text{NO}_3)_2$  as the dopant source. The molar ratios of zinc nitrate were varied from 1, 3, 5, and 7 mM. X-ray diffraction, scanning electron microscopy, and ultraviolet-visible spectroscopy (techniques were employed to characterize the Zn-doped titanium dioxide nanotubes. The samples were then tested in dye-sensitized solar cells, and their photoelectric conversion efficiencies were calculated. As a result, amorphous- $\text{TiO}_2$  structure was transformed into the crystalline anatase phase after annealing. The best performance was observed for the 5 mM zinc nitrate sample, with a photoelectric conversion efficiency of 4.96 % and an energy band gap of 3.18 eV. The findings of this research provide valuable insights for ongoing and future studies in the development of renewable energy.

## KEYWORDS

renewable energy • DSSCs •  $\text{TiO}_2$  nanotubes

**Funding.** The authors would like to greatly thank the following for their support: Thailand Science Research and Innovation Fundamental Fund – FF 2024; the Division of Physics, Faculty of Science, Nakhon Phanom University, Muang District, Nakhon Phanom; and Faculty of Industry and Technology, Rajamangala University of Technology Isan.

**Citation:** Samran B, Timah EN, Phatungthane T, Thongpanit P, Kadroon B, Photharin S, Chaiwichian S. Fabrication and characterization of zinc nitrate doped  $\text{TiO}_2$  nanotubes for dye-sensitized solar cells. *Materials Physics and Mechanics*. 2025;53(5): 83–89.

[http://dx.doi.org/10.18149/MPM.5352025\\_6](http://dx.doi.org/10.18149/MPM.5352025_6)

## Introduction

It was in 1991, when O'Regan and Gratzel [1–3] made their first dye-sensitized solar cells (DSSCs). Since then, there has been huge growth in research on DSSCs. This huge growth can be accounted for due to the following reasons: they are cheap to produce, easy to fabricate, are a source of renewable energy, are environmentally friendly and have high power conversion efficiency [4–10]. Titanium dioxide or titania ( $\text{TiO}_2$ ) nanotubes can be used in DSSCs to improve the photocatalytic performance and resolve the issue of charge recombination [11–14]. However, one challenge encountered with



titania is the large band gap energy of about 3.2 eV. This large band gap restricts solar energy absorption mostly in the UV region. Many reports suggest that this problem can be solved by doping titania with foreign elements. Examples of elements that have been used as dopant in titania include Fe, N, Cu, and Al [15–19].

A.F.Robledo et al.[6], P.Ramos et al. [20] and A. Javed et al. [21] used ZnO nanostructures in DSSCs. Composite nanofibers of ZnO-TiO<sub>2</sub> in DSSCs was reported by C. Qiqi et al. in 2022 [22]. A 1:2 molar ratio of ZnO-TiO<sub>2</sub> was utilized and obtained photoelectric conversion efficiency (PCE) of 3.66 %. There is great room for improvement on this result by doping titania nanotubes (TNT) using zinc nitrate, Zn(NO<sub>3</sub>)<sub>2</sub>, as a source of the dopant element Zn. This research work reports the fabrication and characterization of Zn-doped TNT for DSSCs. The samples were prepared at the molar ratios of zinc nitrate: 1, 3, 5 and 7 mM. The PCE of each sample will be tested in DSSCs.

## Materials and Methods

Direct current (DC) anodization technique was used to develop TNT on titanium sheet from Sigma Aldrich. This process was carried out at a constant voltage supply of 50 V for 2 h at room temperature. The thickness of the each titanium sheet or foil was 0.25 mm thickness and their purity was 99.7 %. The sheets were polished with abrasive paper and degreased by ultrasonic method in isopropanol, deionized water and ethanol. The electrolyte used for the anodization was composed of the following: ethyleneglycol (EG), ammoniumfluoride (0.3 wt. % NH<sub>4</sub>F) and deionized water (2 vol. % D.I. H<sub>2</sub>O). The molar concentrations of zinc nitrate was varied sequentially -1, 3, 5 and 7 mM. To ensure that the electrolyte was homogenous, we kept the mixture for 5 h prior to anodization. The array for the anodization consist of two electrodes – a copper electrode and a platinum counter electrode, as seen in Fig. 1. With this set up, the electrolyte can only be in contact with one face of the titanium sheet.

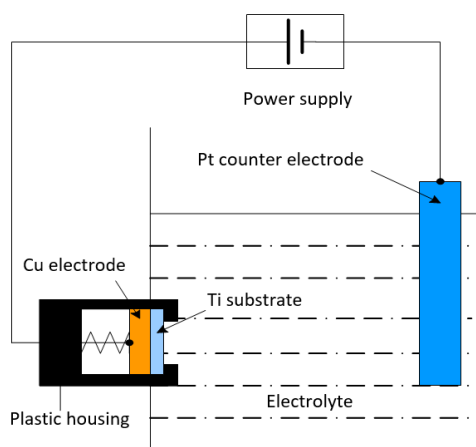


**Fig. 1.** The schematic diagram of a single-face anodization process

Analysis of the samples was performed before calcination and after annealing in an oven at 450 °C. The following techniques were used to characterize the samples: X-ray diffraction (XRD), scanning electron microscopy (SEM), and ultraviolet-visible

spectroscopy (UV-VIS). After that, the samples were tested in DSSCs. To test in DSSCs, the titania nanotubes photoelectrodes were immersed for 24 h at room temperature in 0.5 mM solution of N719 dye and acetonitrile/tert-butanol in a 1:1 mixture. To form the counter electrode, platinum solution ( $H_2PtCl_6$ ) was dropped on a transparent conducting oxide glass (TCO). After heating the TCO at 80 °C for 30 min, the platinum counter electrode was ready. A sandwich assembly of the Pt electrode and the titania nanotube photoelectrode was incorporated into the DSSCs. The current-voltage (IV) characteristic was then analyzed. The following parameters are fundamental in evaluating the photovoltaic properties of the DSSCs: short-circuit current density ( $J_{sc}$ ), open-circuit voltage ( $V_{oc}$ ), fill factor ( $FF$ ) and the photoelectric conversion efficiency PCE ( $\eta$ ). These parameters are related via the equations that follows [23,24]:

$$FF = \frac{V_m I_m}{V_{oc} I_{sc}}, \quad (1)$$

$$\eta = \frac{V_m I_m}{P_{in}} = \frac{V_{oc} I_{sc} FF}{P_{in}}, \quad (2)$$

where  $I_m$  and  $V_m$  are the current and voltage, respectively, at the optimal operating point. Their product gives the maximum output power  $P_m$ . The power of the incident light is denoted as  $P_{in}$ .

## Results and Discussion

### XRD analysis

XRD patterns of the zinc-doped titania nanotubes samples before annealing are displayed in Fig. 2. In Fig. 2, we can see the peaks typical to titanium metal. It is also worth noting that the titania were still in the amorphous phase due to the absence of the anatase phase. On the other hand, Fig. 3 displays XRD patterns after calcinating the samples at 450 °C. It is obvious to see the crystalline anatase phase of  $TiO_2$  which are labelled A. The diffraction peaks for the anatase phase occur at the scattering angles of 25.3, 48.8, 54.2, and 55.1°. These results align perfectly with the works of Hailei Li et al. [25], and Shih-Yu Ho et al. [26].

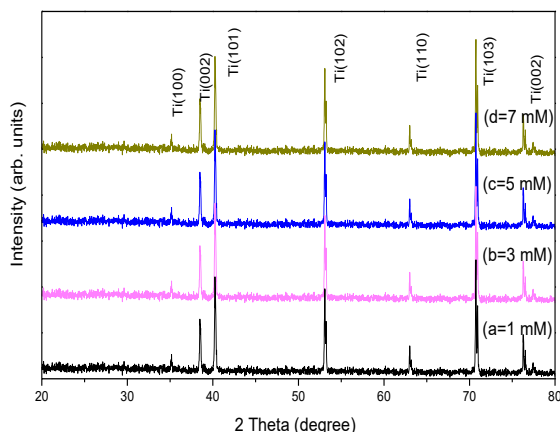


**Fig. 2.** XRD patterns of Zn-doped TNT before annealing: (a) 1 mM, (b) 3 mM, (c) 5 mM, and (d) 7 mM

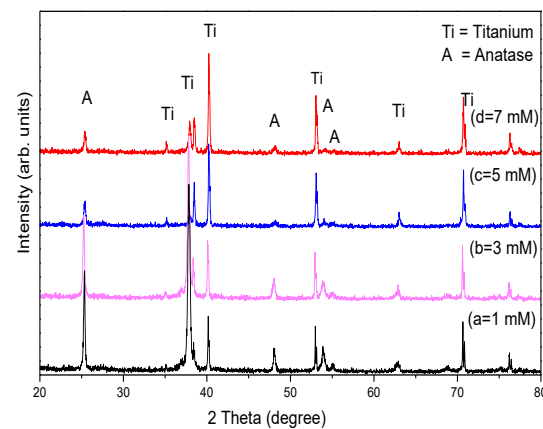


**Fig. 3.** XRD patterns of Zn-doped TNT after annealing at 450 °C: (a) 1 mM, (b) 3 mM, (c) 5 mM and (d) 7 mM

## SEM analysis

The calcinated samples were studied using scanning electron microscopy (SEM). The results presented in Fig. 4 brings to light the changes in the surface morphology of the Zn-doped TNT. The fine structure of the nanotubes gets better with increase in zinc nitrate concentration. However, after 5 mM, the orderliness of the nanotube array is heavily disrupted, as seen with the 7 mM sample. A similar result was obtained by X. Chen et al. [27], when varying the concentrations of HCl.

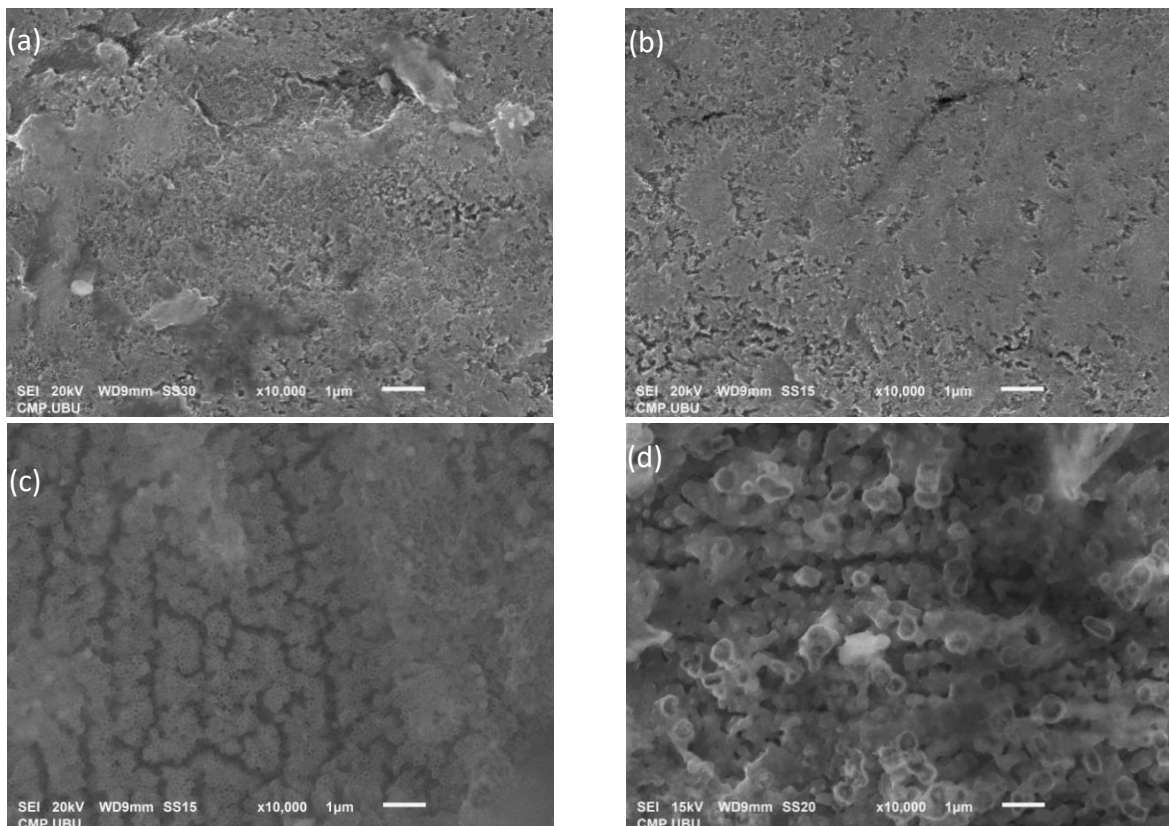


**Fig. 4.** SEM images of Zn-doped TNT after annealing at 450 °C: (a) 1 mM, (b) 3 mM, (c) 5 mM and (d) 7 mM

## UV-visible spectroscopy analysis

The ultraviolet-visible spectrums of the annealed samples are presented in Fig. 5. The sample with a zinc nitrate concentration of 5 mM had the greatest cut off wavelength ( $\lambda_c$ ) of 390 nm.  $\lambda_c$  increased with concentration until 5 mM, and decreased thereafter at the higher concentration of 7 mM. We can attribute this to the disorderly array of the nanotubes demonstrated in SEM images of Fig. 4(d). A large  $\lambda_c$  implies a smaller energy band gap ( $E_g$ ), as demonstrated in Table 1 by Eq. (3) [28–30]:

$$E_g = \frac{hc}{\lambda_c} = \frac{1240}{\lambda_c}, \quad (3)$$

where  $h$  is the Planck constant ( $6.626 \times 10^{-34}$  Js or  $4.14 \times 10^{-15}$  eVs) and  $c$  is the speed of light in vacuum ( $3.00 \times 10^8$  m/s).

**Table 1.** Energy band gap from UV-VIS for different concentrations of Zn-doped TNT after annealing at 450 °C

Samples	1 mM	3 mM	5 mM	7 mM
$\lambda_c$ , nm	379	388	390	384
$E_g$ , eV	3.27	3.20	3.18	3.23

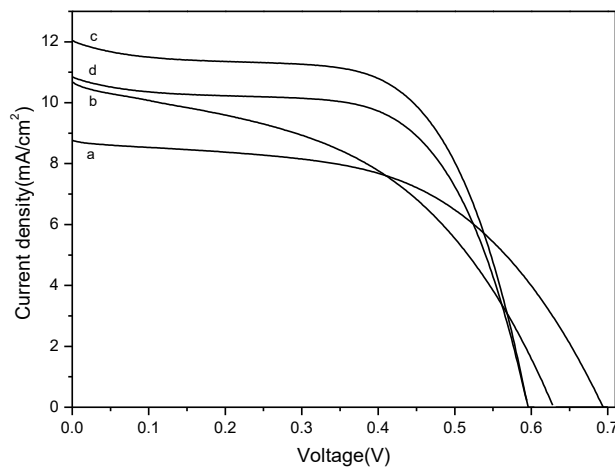


**Fig. 5.** Current-voltage (IV) characteristic curves of Zn-doped TNT after annealing at 450 °C:  
(a) 1 mM, (b) 3 mM, (c) 5 mM and (d) 7 mM

#### IV characteristic and photoelectric performance

Figure 5 and Table 2 both reveal that as zinc nitrate concentration increase, the cell efficiency and photocatalytic performance also increase. One explanation to this is that the dopant element Zn serves as charge traps and helps to reduce charge carrier combination. As more zinc ions replace the titanium ions in the crystal lattice, more charge traps are created. Another reason is that the introduced Zn aid in reducing the band gap energy by forming intermediate energy levels. As a result, the photon absorption of the DSSCs is shifted from the UV region to the Visible light region. This conclusion is supported by the work of Udom T. et al [31]. The 5 mM zinc nitrate sample had the highest PCE of 4.96 %. Because doping reduces the number of trapping states, resulting in a reduction of charge recombination. The efficiency of dye sensitized solar cell of doped Zn- $\text{TiO}_2$  nanotubes obviously declined, which may be due to the formation of recombination centers of photogenerated carriers by the excessive impurity atoms [32]. The cell efficiency at a higher concentration was lower due to a highly distorted and disorganized nanotube array as observed in the SEM images in Fig. 4(d). As a consequence, the charge carrier combination will be greater, resulting in lower PCE and photocatalytic performance.

**Table 2.** Photoelectric performance of Zn-doped TNT after annealing at 450 °C

Samples	$J_{sc}$ , mA/cm <sup>2</sup>	$V_{oc}$ , V	FF	$\eta$ , %
1 mM	8.87	0.68	0.53	3.42
3 mM	10.94	0.64	0.49	3.52
5 mM	12.35	0.62	0.64	4.96
7 mM	10.95	0.61	0.62	3.85

#### Conclusions

Zinc-doped  $\text{TiO}_2$  nanotubes were synthesized by DC anodization at 50 V, and their photocatalytic performance were tested in dye-sensitized solar cells (DSSCs). The

electrolyte was composed of ethyleneglycol (EG), ammoniumfluoride (0.3 % wt NH<sub>4</sub>F), and deionized water (2 % V H<sub>2</sub>O). zinc nitrate was used as the source of the dopant element Zn, and the molar concentrations of zinc nitrate was varied as follows: 1, 3, 5 and 7 mM. The Zn-doped TNT were characterized using several techniques. XRD patterns revealed the transformation of amorphous TiO<sub>2</sub> into the anatase phase after calcination at 450 °C. The surface morphology and array of the nanotubes were studied using SEM. The nanotubes for the 7 mM sample show highly distorted arrangement. The energy band gaps were determined from the UV-VIS results. The lowest band gap energy of 3.18 eV was obtained for the 5 mM sample. This value can be used to account for the optimal photocatalytic performance of the 5 mM sample when tested in DSSCs. It had the highest PCE of 4.96 %. The results of this research provided significant guidelines for ongoing and future research in the development of sustainable energy.

## CRediT authorship contribution statement

**Buagun Samran**  : conceptualization, data curation, investigation, supervision, writing – review & editing, writing – original draft; **Thanatep Phatungthane**  : conceptualization, investigation, supervision, writing – original draft; **Pratya Thongpanit**  : conceptualization, investigation, supervision, writing – original draft; **Bhunpawatana Kadroon**: conceptualization, investigation, supervision, writing – original draft; **Saranyoo Chaiwichian**  : conceptualization, investigation, supervision, writing – original draft, writing – review & editing.

## Conflict of interest

The authors declare that they have no conflict of interest.

## References

1. O'Regan B, Grätzel MA low-cost, high-efficiency solar cell based on dye-sensitized colloidal TiO<sub>2</sub>films. *Nature*. 1991;353: 737–740.
2. Almansour AI, Kumar RS, Al-Shemaimari KI, Arumugam N. Highly Efficient DSSCs Sensitized Using NIR Responsive Bacteriopheophytine-a and Its Derivatives Extracted from Rhodobacter Sphaeroides Photobacteria. *Molecules*. 2024;29(5): 931.
3. Onah EH, Lethole NL, Mukumba P. Luminescent Materials for Dye-Sensitized Solar Cells: Advances and Directions. *Applied Sciences*. 2024;14(20): 9202.
4. Lin C, Liu Y, Wang G, Li K. Novel Dyes Design Based on First Principles and the Prediction of Energy Conversion Efficiencies of Dye-Sensitized Solar Cells. *ACS Omega*. 2021;6(1): 715–722.
5. Radloff GHC, Naba FM, Ocran-Sarsah DB, Bennett ME, Sterzinger KM, Armstrong AT, Layne O, Dawadi MB. Fabrication and characteristics of high efficient dye-sensitized solar cell with composite dyes. *Digest Journal of Nanomaterials and Biostructures*. 2022;17(2): 457–472.
6. Flota Robledo AG, Enríquez JP, Meza Avendaño CA, Pérez Hernández G, Juárez Gutiérrez PJ. DSSCs based on ZnO photoelectrodes sensitized with natural dyes extracted from the bark of Brazil and Taray. *Journal of Optoelectronic and Biomedical Materials*. 2022;14(2): 29–34.
7. Setyawati H, Hadi MS, Darmokoesoemo, H, Murwani IK, Permana AJ, Rochman F. Modification of Methyl Orange dye as a light harvester on solar cell. *IOP Conference Series Earth and Environmental Science*. 2020;456: 012010.
8. Bobyl AV, Davydov RV, Konkov Ol, Kochergin AV, Malevsky DA, Nikitin SE. Accelerated degradation by mechanical load of HIT solar cells encapsulated in flexible plastic. *Material Physics and Mechanics*. 2024;52(4): 1–8.

9. Gusev EYu, Dzhityayeva DZh Yu, Ageyev OA. Effect of PECVD conditions on mechanical stress of silicon films. *Materials Physics and Mechanics*. 2018;37(1): 67–72.
10. VallejoW, Lerma M, Dias-Uribe C. Dye sensitized solar cells: Meta-analysis of effect sensitizer-type on photovoltaic efficiency. *Helyon*. 2025;11(1): e41092.
11. Dholam R, Patel N, Adami M, Miotello M. Hydrogen production by photocatalytic water-splitting using Cr- or Fe-doped  $TiO_2$  composite thin films photocatalyst. *International Journal of Hydrogen Energy*. 2009;34(13): 5337–5346.
12. Liu N, Lee KY, Schmuki P. Small diameter  $TiO_2$  nanotubes vs. nanopores in dye sensitized solar cells. *Electrochemistry Communications*. 2011;15(1): 1873–1902.
13. Park H, Kim WR, Jeong HT, Lee JJ, Kim HG, Choi WY. Fabrication of dye-sensitized solar cells by transplanting highly ordered  $TiO_2$  nanotube arrays. *Solar Energy Materials & Solar Cells*. 2011;95(1):184–189.
14. Chen J, Vishart AL, Sauer SPA, Mikkelsen KV. Teoretical investigations of dye-sensitized solar cells. *Journal of Nanotechnology and Nanomaterials*. 2023;4(2): 38–54.
15. Oviedo AM, Thi HT, Van QC, Nguyen HH. Physicochemical properties of Fe-doped  $TiO_2$  and the application in Dye-sensitized solar cells. *Optical Materials*. 2023;137: 113587.
16. He Z, Que WX, He Y, Hu J, Chen J, Javed HMA, Ji Yu, Li X, Fei D. Electrochemical behavior and photocatalytic performance of nitrogen-doped  $TiO_2$ nanotubes arrays powders prepared by combining anodization with solvothermal process. *Ceramics International*. 2013;39(5):5545–5552.
17. Momeni MM, Ghayeb Y, Ghonchegi Z. Fabrication and characterization of copper doped  $TiO_2$  nanotube arrays by in situ electrochemical method as efficient visible-light photocatalyst. *Ceramics International*. 2015;41(7):8735–8741.
18. Samran B, Phatungthane T, Timah E, Tipparach U. Synthesis of Aluminum-Doped  $TiO_2$ Nanotubes by Anodization Method. *Key Engineering Materials*. 2017;728: 209–214.
19. Rahman S, Haleem A, Siddiq M, Hussain MK, Qamar S, Hameed S, Waris M. Research on dye sensitized solar cells: recent advancement toward the various constituents of dye sensitized solar cells for efficiency enhancement and future prospects. *RSC Advances*. 2023;28: 19508.
20. Ramos P, Flores G, Sánchez E, Candal LA, Hojamberdiev RJ, Estrada M, Rodriguez W. Enhanced photoelectrochemical performance and photocatalytic activity of  $ZnO/TiO_2$  nanostructures fabricated by an electrostatically modified electrospinning. *Applied Surface Science*. 2017;426: 844–851.
21. Javed AH,Shahzad N, Khan AM, Ayub M, Iqbal N, Hassan M, Hussain N, Rameel MI, Shahzad MI. Effect of  $ZnO$  nanostructures on the performance of dye sensitized solar cells. *Solar Energy*. 2021;230: 492–500.
22. Chang Q, Xu J, Han Y, Ehrmann A, He TH, Zheng RP. Photoelectric Performance Optimization of Dye-Sensitized Solar Cells Based on  $ZnO-TiO_2$  Composite Nanofibers. *Journal of Nanomaterials*. 2022;2022(1): 7356943.
23. Li S, Liu YM, Zhang G, Zhao XZ, Yin J. The role of the  $TiO_2$ nanotube array morphologies in the dye-sensitized solar cells. *Thin Solid Films*. 2011;520(2): 689–693.
24. Kim SS, Yum JH, Sung YE. Improved performance of a dye-sensitized solar cell using a  $TiO_2/ZnO/Eosin Y$  electrode. *Solar Energy Materials & Solar Cells*. 2003;79(4): 495–505.
25. Li H, Cao L, Liu W, Su G, Dong B. Synthesis and investigation of  $TiO_2$ nanotube arrays prepared by anodization and their photocatalytic activity. *Ceramics International*. 2012;38(7): 1–4.
26. Ho SY, SuC, Kathirvel S, Li CY, Li WR. Fabrication of  $TiO_2$ nanotube–nanocube array composite electrode for dye-sensitized solar cells. *Thin Solid Films*. 2013;529: 123–127.
27. Chen X, Schriver M, Suen T, Mao SS. Fabrication of 10 nm diameter  $TiO_2$ nanotube arrays by titanium anodization. *Thin Solid Films*. 2007;515(24): 8511–8514.
28. Yathisha RO, Nayaka YA. Optical andelectrical properties oforganic dye sensitized Cr–ZnO andNi–CdO nanoparticles. *SN Applied Sciences*. 2020;2: 451.
29. Guo W, Ye J, Chang H, Yu C. Damage Characteristics Analysis of Laser Ablation Triple-Junction Solar Cells Based on Electroluminescence Characteristics. *Sensors*. 2024;24(15): 4886.
30. Miah MH, Khandaker MU, Rahman MB, Alam MNE, Islam MA. Band gap tuning of perovskite solar cells for enhancing the efficiency and stability: issues and prospects. *RSC Advances*. 2024;14: 15876–15906.
31. Tipparach U, Wongwanwatthana P, Sompan T, Saipin T, Krongkitsiri P. Preparation and Characterization of Nano- $TiO_2$  Thin Films by Sol-gel Dip-coating Method. *Chiang Mai University Journal of Natural Sciences. Special Issue on Nanotechnology*. 2008;7(1): 129–136.
32. Jiang K, Zhang J, Luo R, Wan Y, Liu Z, Chen J. A facile synthesis of Zn-doped  $TiO_2$  nanoparticles with highly exposed (001) facets for enhanced photocatalytic performance. *RSC Advances*. 2021;11: 7627–7632.